ISBN: 978-3-95450-184-7 doi:10.18429/JACoW-IPAC2018-WEPML026

LARGE-APERTURE HIGH-FIELD Nb_3Sn DIPOLE MAGNETS*

A.V. Zlobin†, V.V. Kashikhin, I. Novitski, Fermilab, 60510 Batavia, U.S.A.

Abstract

Large-aperture high-field dipole magnets based on Nb_3Sn superconductor are necessary for various accelerator systems of future hadron and muon colliders. High magnetic fields and large apertures lead to large Lorentz forces and mechanical strains and stresses which can damage brittle Nb_3Sn coils. This paper describes conceptual designs of 120-mm aperture dipoles with magnetic fields up to 15 T based on cos-theta coils and a stress management technique.

INTRODUCTION

Nb_3Sn accelerator magnet technology has made significant progress in the past decade. Therefore, Nb_3Sn dipoles and quadrupoles with a nominal field of 11-12 T are being considered in the near future for the LHC luminosity upgrade (HL-LHC project) [1]. In the longer term, cost-effective 15-16 T Nb_3Sn magnets will be needed for the LHC energy upgrade (HE-LHC) or the Future Circular Collider (FCC) [2].

Large-aperture high-field dipole magnets based on Nb_3Sn superconductor are essential for various accelerator systems of future hadron and muon colliders. In hadron colliders, they are needed for beam separation before and after the interaction points [3]. In a muon collider, they are considered for both the arc and the interaction regions to provide room for thick internal absorbers protecting magnets from muon decay products [4, 5]. Such magnets can also be used in test facilities to provide a background magnetic field for testing conductor samples or insert coils [6].

High magnetic fields and large apertures lead to large Lorentz forces and mechanical strains and stresses which can damage brittle Nb_3Sn coils. Magnet design studies are being performed in the framework of the U.S. Magnet Development Program (MDP) [7] to explore the limits of the Nb_3Sn accelerator magnet technology in general and the feasibility and limits of large-aperture magnets as outserts for a 20 T HTS/LTS dipole (MDP) in particular. A preliminary analysis shows that a 120-mm aperture is acceptable for this purpose. This paper describes conceptual designs and parameters of 120-mm aperture Nb_3Sn dipoles based on cos-theta coils with stress management. The stress management (SM) technique and limits are also presented and discussed.

MAGNET DESIGN AND PARAMETERS

The first design of a large-aperture dipole (Design 1), considered in this study, is based on the two outermost layers of the 17 T 60-mm aperture dipole described in [8]. The 2-layer outer coil has a 120 mm aperture and uses a stress management concept. Each layer consists of 5 blocks placed inside a slotted stainless steel structure with 5-mm thick radial and azimuthal walls. The coil is wound using a 40-strand Rutherford cable with 0.7 mm Nb_3Sn strands.

The second design (Design 2) also has a 120-mm aperture and a 4-layer graded coil with a similar stress management concept as Design 1. All pole blocks are made of Ti alloy and are installed into the structure before winding. The 2-layer inner coil has 5 blocks in each layer wound from a 28-strand Rutherford cable with 1 mm Nb_3Sn strands. The 2-layer outer coil has 5 blocks in the inner layer and 4 blocks in the outer layer. Both layers are wound as in Design 1 from the Rutherford cable with 40-strands, each 0.7 mm in diameter. The cross-sections of 2-layer (Design 1) and 4-layer (Design 2) coils with stress management are shown in Fig. 1.

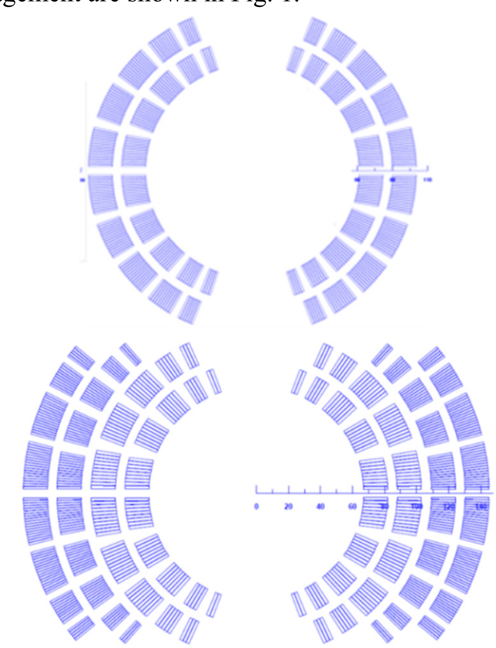

Figure 1: Cross-sections of Design 1 and Design 2 coils with 120-mm aperture.

The 28-strand and 40-strand cables are 15.1 mm wide, have a keystoned cross-section with a keystone angle of 0.805 degree, and use Nb_3Sn strands with a Cu/non-Cu ratio of 1.13 and critical current density J_c at 15 T and 4.2 K of 1500 A/mm^2. The mid-thickness of the 28-strand and 40-strand cables is 1.870 mm and 1.319 mm respectively.

Both designs were studied using ROXIE code [9]. The magnetic model included a cylindrical iron yoke with an outer diameter of 700 mm and a realistic B(H) curve. The main magnet parameters are summarized in Table 1 for a Nb_3Sn cable J_c of 1.5 kA/mm^2 at 15 T and 4.2 K, which corresponds to 3.0 kA/mm^2 at 12 T and 4.2 K.

* Work is supported by Fermi Research Alliance, LLC, under contract No. DE-AC02-07CH11359 with the U.S. Department of Energy
† zlobin@fnal.gov

ISBN: 978-3-95450-184-7 doi:10.18429/JACoW-IPAC2018-WEPML026

Table 1: Magnet Parameters at SSL and 4.2 K

Parameter	Design 1	Design 2
Number of layers	2	4
Bore field, T	12.10	15.42
Peak field, T	14.18	15.88
Current, A	13.06	12.50
Inductance, mH/m	22.47	64.94
Stored energy, MJ/m	1.92	5.07
F_x, MN/m/quadrant	7.59	12.38
F_y, MN/m/quadrant	-3.17	-8.01

The maximum bore field in Design 1 at 4.2 K is 12.1 T, whereas in Design 2 it is 15.4 T. Note that since the coil cross-section was not optimized for field quality, the bore field in Design 1 is 18% lower than the peak field. In Design 2, the bore field is only 3% lower than the peak field due to a more optimum coil geometry. The sensitivity of bore field to magnet operation temperature and superconductor critical current density J_c at 12 T and 4.2 K is shown in Fig. 2. It can be seen that variations of the conductor critical current density within 50% changes the bore field by only ~10% for Design 1 and by ~8.5% for Design 2.

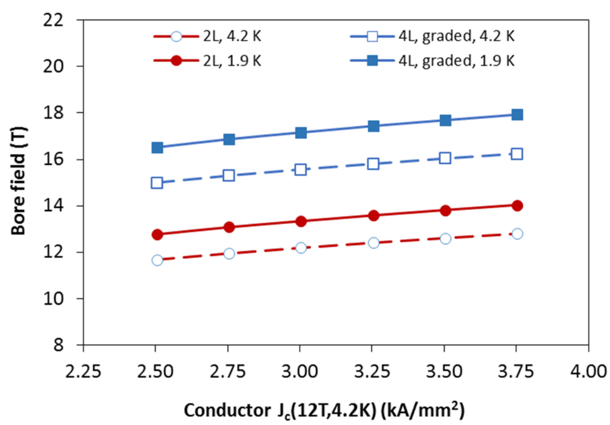

Figure 2: Maximum field in magnet aperture vs. conductor critical current density J_c at 12 T and 4.2 K.

MECHANICAL ANALYSIS

To investigate the limitations related to the large Lorentz forces, a mechanical analysis was performed using ANSYS code and parametric models. The coil blocks are integrated into the stainless steel structure with 5 mm thick radial and azimuthal spacers and separated pole blocks. The coil blocks are allowed to separate from the structure to capture the effect of unloading under Lorentz forces. In addition, each layer could slide with respect to the adjacent layers and to the iron yoke. It was also assumed that the vertical gap in the iron yoke remains closed at all fields. The coils were pre-compressed during assembly by placing appropriate radial shims between the inner and outer coils and between the outer coil and the iron yoke.

The goal of the mechanical analysis was to find the maximum field for each design at which a) the maximum stress in the coil does not exceed the acceptable stress for brittle Nb_3Sn coils of ~200 MPa at operation temperatures, and b) the separations of the coil blocks from the structure in the azimuthal direction are small, and the length of separation areas is less than the cable width. Results of the analysis have shown that for Design 1 this field is ~11 T and for Design 2 it is ~15 T.

Calculated distributions of the equivalent stress in the Design 1 and Design 2 coils after cool-down and at the corresponding maximum field (11 T for Design 1 and 15 T for Design 2) are shown in Figs. 3 and 4. In both designs, the peak equivalent stress in the coil after cool-down is in the pole blocks of layer 1. It reaches 185 MPa in Design 1 and 190 MPa in Design 2. In both designs, due to the azimuthal component of the Lorentz force, at the maximum field turns in each block shift towards the coil midplane. In Design 1 at a bore field of 11 T the maximum equivalent stress in the coil is ~155 MPa, and in Design 2 at 15 T it is ~190 MPa.

Lorentz forces push turns in each block towards the coil mid-plane. Under certain conditions they may separate from the support structure. In Design 1 at a bore field of 11 T, small gaps up to 4 µm with lengths smaller than 30% of the cable width are seen in the two coil blocks of the outer-layer next to the pole. In Design 2, at 15 T the larger gaps up to 25 µm and with lengths up to 50% of the cable width are in the 2-3 pole blocks in each layer.

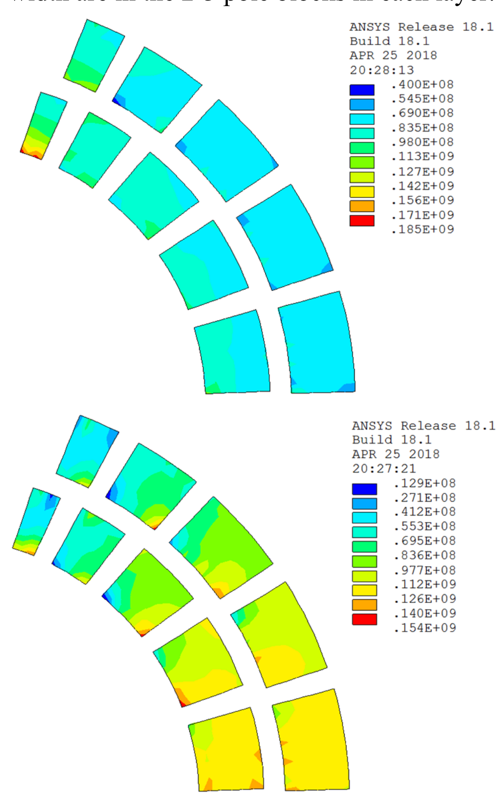

Figure 3: The coil equivalent stress (Pa) after cool-down (top) and at the bore field of 11 T (bottom) of Design 1.

ISBN: 978-3-95450-184-7 doi:10.18429/JACoW-IPAC2018-WEPML026

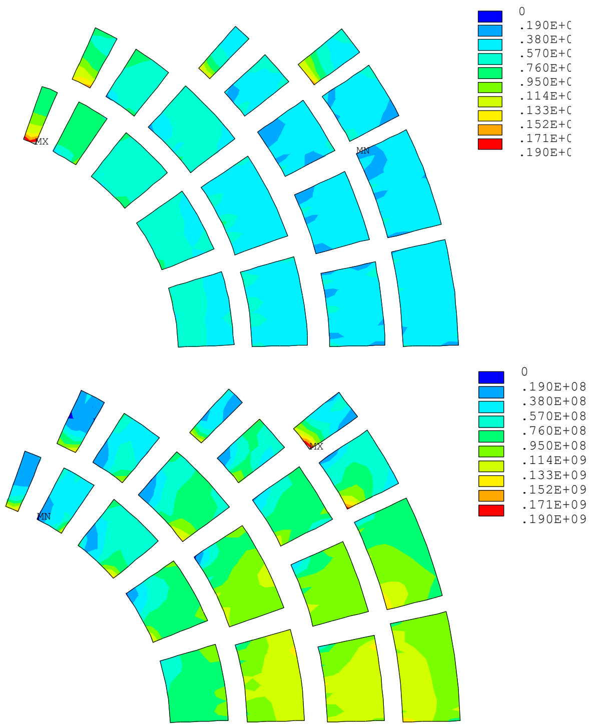

Figure 4: The coil equivalent stress (Pa) after cool-down (top) and at the bore field of 15 T (bottom) of Design 2.

Calculated distributions of the equivalent stress in the coil structure after cooling-down and at the maximum bore field in the two designs are shown in Figs. 5 and 6.

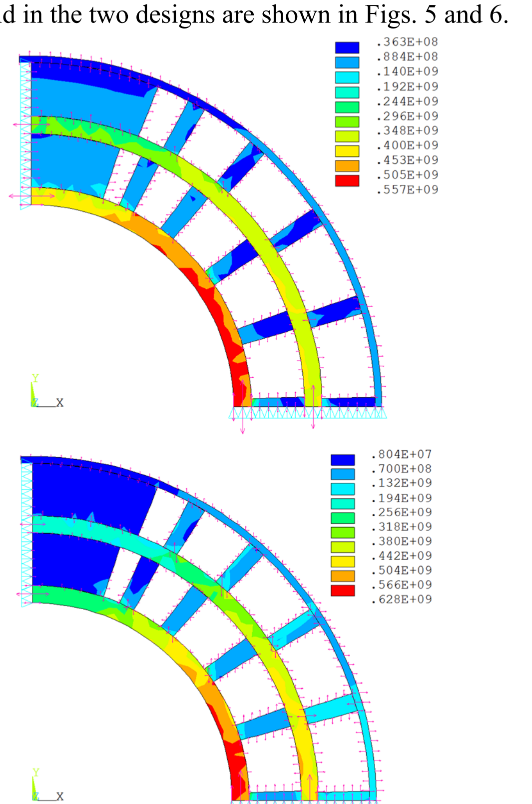

Figure 5: Equivalent stress (Pa) in the coil support structure of Design 1 after cool-down (top) and at 11 T bore field (bottom).

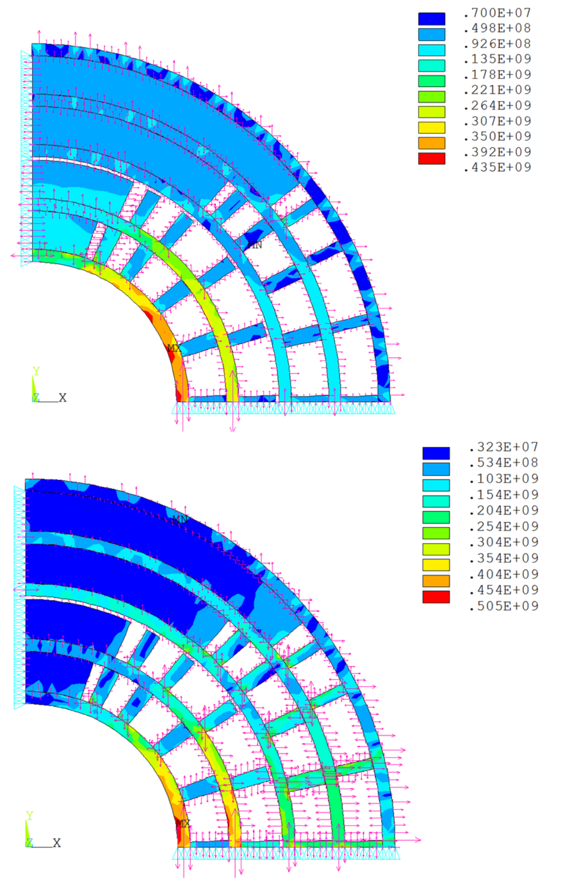

Figure 6: Equivalent stress (Pa) in the coil support structure of Design 2 after cool-down (top) and at 15 T bore field (bottom).

In both designs the maximum equivalent stress is located near the midplane of the innermost radial wall of the coil support structure. In Design 1 the maximum equivalent stress is ~550 MPa after cool-down and ~630 MPa at the maximum bore field of 11 T. In design 2 it is 435 MPa and 505 MPa respectively.

CONCLUSION

Nb_3Sn dipole designs with 2-layer and 4-layer coils with 120-mm free aperture and stress management have been analyzed. Although the magnet conductor limit for state-of-the-art Nb_3Sn composite wires is quite high, up to 13 T in the 2-layer design and up to ~17 T in the 4-layer design at 1.9 K, the magnet design field is limited to 11 T and 15 T respectively by mechanical considerations. Optimization of coil and stress management structure will continue to extend the operation field range in 120-mm aperture dipole magnets.

REFERENCES

[1] G. Ambrosio, "Nb_3Sn High Field Magnets for the High-Luminosity LHC Upgrade Project," IEEE Trans. on Appl. Supercond., vol. 25(3), 2015, 4002107.

ISBN: 978-3-95450-184-7 doi:10.18429/JACoW-IPAC2018-WEPML026

[2] D. Tommasini *et al.*, "The 16 T Dipole Development Program for FCC," IEEE Trans. on Appl. Supercond., vol. 27(4), 2017.

[3] J.B. Strait *et al.*, "Towards a New LHC Interaction Region Design for a Luminosity Upgrade," in PAC'03, Portland, OR, USA, May 2003, pp. 42-44.

[4] V.V. Kashikhin *et al.*, "High-Field Combined Function Magnets for a 1.5×1.5 TeV Muon Collider Storage Ring," at IPAC2012, New Orleans, USA, May 2012, pp. 3587-3589.

[5] A.V. Zlobin *et al.*, "Storage Ring and Interaction Region Magnets for a $\mu^+\mu^-$ Higgs Factory," in NAPAC'13, Pasadena, CA, USA, Sep.-Oct. 2013, paper THPBA19, pp. 1271-1273.

[6] P. Ferracin *et al.*, "Development of the EuCARD Nb_3Sn Dipole Magnet FRESCA2," IEEE Trans. on Appl. Supercond., vol. 23(3), 2013, 4002005.

[7] S.A. Gourlay *et al.*, "The U.S. Magnet Development Program Plan," 16-AT-2934, LBNL-100646, 2016/6/1.

[8] A.V. Zlobin *et al.*, "Conceptual Design of a 17 T Nb_3Sn Dipole Magnet," presented at IPAC'18, Vancouver, Canada, Apr.-May 2018, paper WEPML027, this conference.

[9] *ROXIE* code for electromagnetic simulations and optimization of accelerator magnets, http://cern.ch/roxie